JOC The Journal of Organic Chemistry

Article

pubs.acs.org/joc

A Kinetic Study on Nucleophilic Displacement Reactions of Aryl Benzenesulfonates with Potassium Ethoxide: Role of K^+ Ion and Reaction Mechanism Deduced from Analyses of LFERs and Activation Parameters

Ik-Hwan Um,*[,†] Ji-Sun Kang,[†] Young-Hee Shin,[†] and Erwin Buncel[‡]

[†]Department of Chemistry and Nano Science, Ewha Womans University, Seoul 120-750, Korea

[‡]Department of Chemistry, Queen's University, Kingston, Ontario K7L 3N6, Canada

Supporting Information

ABSTRACT: Pseudofirst-order rate constants (k_{obsd}) have been measured spectrophotometrically for the nucleophilic substitution reactions of 2,4-dinitrophenyl X-substituted benzenesulfonates **4a**−**f** and Y-substituted phenyl benzenesulfonates **5a**−**k** with EtOK in anhydrous ethanol. Dissection of k_{obsd} into k_{EtO^-} and k_{EtOK} (i.e., the second-order rate constants for the reactions with the dissociated EtO^- and ion-paired EtOK, respectively) shows that the ion-paired EtOK is more reactive than the dissociated EtO^-, indicating that K^+ ion catalyzes the reaction. The catalytic effect exerted by K^+ ion (e.g., the k_{EtOK}/k_{EtO^-} ratio) decreases linearly as the substituent X in the benzenesulfonyl moiety changes from an electron-donating group (EDG) to an electron-withdrawing group (EWG), but it is independent of the electronic nature of the substituent Y in the leaving group. The reactions have been concluded to proceed through a concerted mechanism from analyses of the kinetic data through linear free energy relationships (e.g., the Brønsted-type, Hammett, and Yukawa−Tsuno plots). K^+ ion catalyzes the reactions by increasing the electrophilicity of the reaction center through a cyclic transition state (TS) rather than by increasing the nucleofugality of the leaving group. Activation parameters (e.g., $\Delta H^{\ddagger}$ and $\Delta S^{\ddagger}$) determined from the reactions performed at five different temperatures further support the proposed mechanism and TS structures.

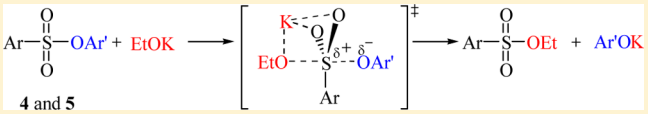

INTRODUCTION

Metal ions have often been reported to catalyze acyl-group transfer reactions as a Lewis acid catalyst.[1−10] Since Lewis acidity increases as the charge density of metal ions increases, studies have focused mostly on the reactions involving multivalent metal ions (e.g., La^{3+}, Eu^{3+}, Co^{3+}, Zn^{2+}, Cu^{2+}, Mn^{2+}, etc.).[1−5] It is well-known that alkali-metal ions are ubiquitous in nature and play important roles in biological processes (e.g., the Na^+/K^+ pump to maintain high K^+ and low Na^+ concentrations in mammalian cells).[11] Nevertheless, the effect of alkali-metal ions on acyl-group transfer reactions has much less been investigated.

The first kinetic study on the effect of alkali-metal ions was performed by our group for the phosphinyl-transfer reaction of 4-nitrophenyl diphenylphosphinate **1a** with alkali metal ethoxides (EtOM, M = Li, Na, and K) in anhydrous ethanol.[6a] The study has shown that M^+ ions catalyze the reaction but the catalytic effect disappears in the presence of complexing agents for M^+ ions, e.g., 18-crown-6-ether (18C6) or cryptands.[6a] Besides, the catalytic effect has been found to increase as the size of M^+ ions decreases (i.e., $K^+ < Na^+ < Li^+$).[6a] In contrast, we have recently reported that the reaction of 4-nitrophenyl diphenylphosphinothioate **1b** with EtOM is inhibited by Li^+ ion but is catalyzed by Na^+ and K^+ ions.[9] More interestingly, the K^+ ion complexed by 18C6 exhibited stronger catalytic effect than Na^+ or K^+ ion,[9] indicating that the role of M^+ ions is strongly dependent on the nature of the electrophilic center (P═O vs P═S).

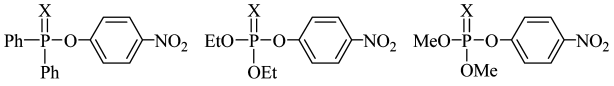

A similar result has been reported for the phosphoryl-transfer reactions of ethyl paraoxon **2a** and methyl paraoxon **3a** with EtOM and the corresponding reactions of ethyl parathion **2b** and methyl parathion **3b**; i.e., (1) the reaction of the P═O compounds **2a** and **3a** is catalyzed by M^+ ions in the order $K^+ < Na^+ < Li^+$, (2) the reaction of the P═S compound **2b** is catalyzed by K^+ ion but inhibited by Na^+ and Li^+ ions, and (3) the reaction of the P═S compound **3b** is strongly catalyzed by 18C6-complexed K^+ ion but inhibited by Na^+ and Li^+ ions.[10] The contrasting M^+ ion effects were discussed on the basis of competing electrostatic effects and solvational requirements as function of anionic electrophilic field strength and cationic size (Eisenman's theory).[12]

The effect of M^+ ions on sulfonyl-transfer reactions has also been investigated. We have reported that the reaction of Y-

Received: October 25, 2012
Published: December 10, 2012

   dx.doi.org/10.1021/jo302373y | J. Org. Chem. 2013, 78, 490−497

substituted phenyl benzenesulfonates (Y = 4-NO_2, 3-NO_2, 4-CF_3, 3-Br, 4-Cl, and H) with EtOM is catalyzed by K^+ ion but inhibited by Li^+ ion.[13] The reaction was suggested to proceed through a stepwise mechanism, in which formation of the EtO−S bond is well advanced in the rate-determining transition state (TS), while breakdown of the S−OAr bond is negligible on the basis of the kinetic results that σ° constants result in much better Hammett correlation than σ^- constants.[13] Accordingly, it has been concluded that K^+ ion catalyzes the reaction by stabilizing the TS through TS_1, in which K^+ ion increases the electrophilicity of the sulfonyl sulfur.[13] However, a possibility that K^+ ion catalyzes the reaction by increasing the nucleofugality of the leaving group cannot be excluded, if breakdown of the S−OAr bond is involved in the rate-determining step (RDS). Thus, more detailed information on the reaction mechanism including the TS structure is necessary to understand the role of K^+ ion.

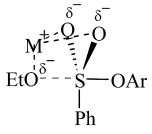

TS_1

We have now carried out a systematic study on the reaction of 2,4-dinitrophenyl X-substituted benzenesulfonates **4a**−**f** and Y-substituted phenyl benzenesulfonates **5a**−**k** with EtOK to revisit the role of K^+ ion as well as the reaction mechanism (Scheme 1). We have introduced various substituents on the nonleaving sulfonyl moiety as well as on the leaving aryloxide. Moreover, activation parameters (i.e., $\Delta H^{\ddagger}$ and $\Delta S^{\ddagger}$) have been measured to get further information on the TS structures. Analysis of the current kinetic data through linear free energy relationships (e.g., Brønsted-type, Hammett, and Yukawa−Tsuno plots) has led us to conclude that the reaction proceeds through a concerted mechanism, in which K^+ ion catalyzes the reaction by increasing the elctrophilicity of the reaction center rather than by increasing the nucleofugality of the leaving aryloxide. The activation parameters (i.e., $\Delta H^{\ddagger}$ and $\Delta S^{\ddagger}$) determined from the reactions performed at 5 different temperatures further support the proposed mechanism and TS structures.

Scheme 1

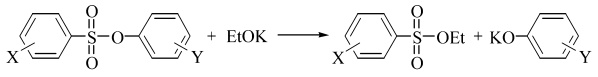

4 and **5**

Y= 2,4-$(NO_2)_2$; X= 4-MeO (**4a**), 4-Me (**4b**), H (**4c**), 4-Cl (**4d**), 3-NO_3 (**4e**), 4-NO_2 (**4f**).

X= H ; Y= 2,4-$(NO_2)_2$ (**5a**), 3,4-$(NO_2)_2$ (**5b**), 4-NO_2 (**5c**), 4-CHO (**5d**), 2,4-Cl_2 (**5e**), 4-CN (**5f**), 4-COMe (**5g**), 4-CF_3 (**5h**), 3-Br (**5i**), 4-Cl (**5j**), H (**5k**).

RESULTS AND DISCUSSION

The reactions were followed spectrophotometrically by monitoring the appearance of the leaving Y-substituted phenoxide ion under pseudofirst-order conditions with large excess of EtOK. All reactions in the current study obeyed pseudofirst-order kinetics. Pseudofirst-order rate constant (k_{obsd}) was calculated from the slope of the linear plot of ln ($A_\infty - A_t$) vs t. The correlation coefficients of the linear plots were higher than 0.9995. The uncertainty in the k_{obsd} values is estimated to be less than ±3% from replicate runs. The k_{obsd} values and detailed kinetic conditions for the reactions of 2,4-dinitrophenyl benzenesulfonates (**4a**−**f**) and Y-substituted phenyl benzenesulfonates (**5a**−**k**) are summarized in Tables S1−S23 in the Supporting Information (SI).

As shown in Figure 1, the plot of k_{obsd} vs [EtOK] for the reaction of 2,4-dinitrophenyl 4-methoxybenzenesulfonate (**4a**)

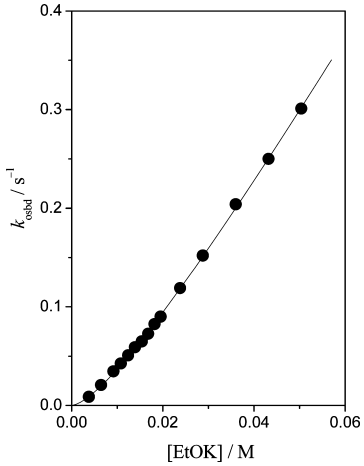

Figure 1. Plot of k_{obsd} vs [EtOK] for the reaction of 2,4-dinitrophenyl 4-methoxybenzenesulfonate **4a** with EtOK in anhydrous EtOH at 25.0 ± 0.1 °C. The curved line was calculated by eq 2.

with EtOK curves upward. Similarly curved plots are illustrated in Figures S6A−S10A in the SI for the reactions of 2,4-dinitrophenyl X-substituted benzenesulfonates (**4b**−**f**), and in Figures S11A−S27A (SI) for those of Y-substituted phenyl benzenesulfonates (**5a**−**k**). It is noted that such upward curvature illustrated in the plots of k_{obsd} vs [EtOK] is typical of reactions of esters with EtOM (M = K, Na, and Li), in which the ion-paired EtOM was reported to be more reactive than the dissociated EtO^-.[6]

Dissection of k_{obsd} into k_{EtO^-} and k_{EtOK}. To confirm that the ion-paired EtOK is more reactive than the dissociated EtO^-, the k_{obsd} values for the reactions of **4a**−**f** have been dissected into k_{EtO^-} and k_{EtOK}, i.e., the second-order rate constants for the reactions with the dissociated EtO^- and ion-paired EtOK, respectively. EtOM was reported to exist as a dimer or other aggregates in a high concentration region (e.g., [EtOM] > 0.1 M) but was suggested to exist as the dissociated and ion-paired species in concentrations below 0.1 M.[14] Since the reactions in this study were carried out in a low concentration region (e.g., [EtOK] < 0.1 M), EtOK would exist as the dissociated EtO^- and ion-paired EtOK. Accordingly, both the dissociated EtO^- and ion-paired EtOK would react with the substrate with rate constants k_{EtO^-} and k_{EtOK}, respectively, as shown in Scheme 2.

A rate eq 1 can be derived on the basis of the reactions proposed in Scheme 2. Under a pseudofirst-order kinetic condition, k_{obsd} can be expressed as eq 2. Since the dissociation constant $K_d = [EtO^-]_{eq}[K^+]_{eq}/[EtOK]_{eq}$, and $[EtO^-]_{eq} = [K^+]_{eq}$ at equilibrium, eq 2 becomes eq 3. The concentrations of $[EtO^-]_{eq}$ and $[EtOK]_{eq}$ can be calculated from the previously reported K_d value (i.e., $K_d = 1.11 \times 10^{-2}$ M for EtOK)[15] and the total concentration of EtOK (i.e., [EtOK]) using eqs 4 and 5.

dx.doi.org/10.1021/jo302373y | J. Org. Chem. 2013, 78, 490−497

Scheme 2

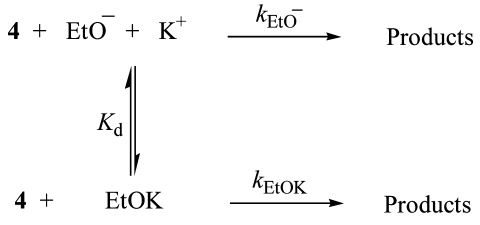

$$\text{rate} = k_{EtO^-}[EtO^-]_{eq}[\mathbf{4}] + k_{EtOK}[EtOK]_{eq}[\mathbf{4}] \quad (1)$$

$$k_{obsd} = k_{EtO^-}[EtO^-]_{eq} + k_{EtOK}[EtOK]_{eq} \quad (2)$$

$$k_{obsd}/[EtO^-]_{eq} = k_{EtO^-} + k_{EtOK}[EtO^-]_{eq}/K_d \quad (3)$$

$$[EtOK] = [EtO^-]_{eq} + [EtOK]_{eq} \quad (4)$$

$$[EtO^-]_{eq} = [-K_d + (K_d^2 + 4K_d[EtOK])^{1/2}]/2 \quad (5)$$

One might expect that the plot of $k_{obsd}/[EtO^-]_{eq}$ vs $[EtO^-]_{eq}$ is linear with a positive intercept, if the reaction proceeds as proposed in Scheme 2. In fact, Figure 2 shows that the plot is linear with a positive intercept for the reaction of **4a**. Similarly linear plots are illustrated for the reactions of **4b–f** in Figures S6B–S10B in the SI, indicating that the above equations derived from the reactions proposed in Scheme 2 are indeed correct. Thus, the k_{EtO^-} and k_{EtOK}/K_d values have been calculated from the intercept and the slope of the linear plots, respectively. The k_{EtOK} value can be calculated from the k_{EtOK}/K_d ratios determined above and the previously reported K_d value.[15] The k_{EtO^-} and k_{EtOK} values calculated in this way are summarized in Table 1 for the reaction of **4a–f** together with the k_{EtOK}/k_{EtO^-} ratios. The effect of substituent X on the reactivity and reaction mechanism will be discussed subsequently.

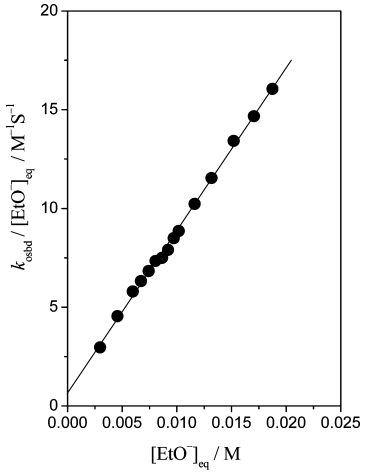

Figure 2. Plot of $k_{obsd}/[EtO^-]_{eq}$ vs $[EtO^-]_{eq}$ for the reaction of 2,4-dinitrophenyl 4-methoxybenzenesulfonate **4a** with EtOK in anhydrous EtOH at 25.0 ± 0.1 °C.

Effect of Substituent X on Reactivity and Reaction Mechanism. As shown in Table 1, the reactivity of **4a–f** toward the dissociated EtO^- increases as the substituent X in the benzenesulfonyl moiety changes from an electron-donating group (EDG) to an electron-withdrawing group (EWG); e.g., k_{EtO^-} increases from 0.624 M^{-1} s^{-1} to 5.82 and 780 M^{-1} s^{-1} as the substituent X changes from 4-MeO to H and 4-NO_2, in turn. A similar result is demonstrated for the reactions with the ion-paired EtOK, although $k_{EtOK} > k_{EtO^-}$ regardless of the electronic nature of the substituent X. This confirms that the ion-paired EtOK is more reactive than the dissociated EtO^-. It is noted that the catalytic effect exerted by K^+ ion (i.e., the k_{EtOK}/k_{EtO^-} ratio) decreases linearly as the substituent X changes from an EDG to an EWG (see also Figure S1 in the SI).

Table 1. Summary of the Kinetic Data for the Reactions of 2,4-Dinitrophenyl X-Substituted Benzenesulfonates 4a–f with EtOK in Anhydrous EtOH at 25.0 ± 0.1 °C

entry	X	k_{EtO^-}/M^{-1} s^{-1}	k_{EtOK}/M^{-1} s^{-1}	k_{EtOK}/k_{EtO^-}
4a	4-MeO	0.624 ± 0.100	9.16 ± 0.10	14.7
4b	4-Me	1.53 ± 0.20	20.2 ± 0.2	13.2
4c	H	5.82 ± 0.40	40.6 ± 0.4	6.98
4d	4-Cl	19.9 ± 3.0	109 ± 3	5.48
4e	3-NO_2	505 ± 20	1470 ± 19	2.91
4f	4-NO_2	780 ± 30	1740 ± 27	2.23

The effect of substituent X on the reactivity of the dissociated EtO^- and ion-paired EtOK is illustrated in Figure 3. The Hammett plots for the reactions of **4a–f** with the dissociated EtO^- and ion-paired EtOK exhibit excellent linear correlations with large slopes, i.e., ρ_X = 2.89 and 2.15 for the reactions with EtO^- and EtOK, respectively. The ρ_X values obtained for the current reactions are comparable with those reported previously for reactions of esters with anionic nucleophiles (e.g., ρ_X = 2.90 ± 0.05 for the reactions of 4-nitrophenyl X-substituted benzoates with EtO^- and $C_6H_5O^-$ ions,[16] and ρ_X = 2.28 for the reactions of *O*-4-nitrophenyl X-substituted thionobenzoates with N_3^- ion[17]) but are much larger than those reported for the reactions with neutral amines (e.g., ρ_X = 0.58 for the reactions of **4a–f** with piperidine,[18] and ρ_X = 0.42–0.75 for the reactions of 4-nitrophenyl X-substituted benzoates with various amines[19]). The large positive ρ_X values obtained in the current reactions suggest that the negative charge developed in the sulfonyl moiety of the TS is significant. However, the current Hammett plots alone are not sufficient to

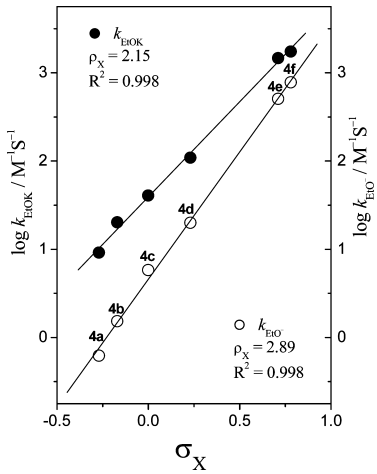

Figure 3. Hammett plots for the reactions of 2,4-dinitrophenyl X-substituted benzenesulfonates **4a–f** with the dissociated EtO^- (○) and ion-paired EtOK (●) in anhydrous EtOH at 25.0 ± 0.1 °C. The identity of the points is given in Table 1.

dx.doi.org/10.1021/jo302373y | J. Org. Chem. 2013, 78, 490–497

conclude whether the reactions proceed through a concerted mechanism or through a stepwise pathway.

Effect of Substituent Y on Reactivity and Reaction Mechanism. To obtain more conclusive information on the reaction mechanism, the kinetic study has been extended to the reactions of Y-substituted phenyl benzenesulfonates **5a–k**. The second-order rate constants k_{EtO^-} and k_{EtOK} are summarized in Table 2 together with the k_{EtOK}/k_{EtO^-} ratios. It can be observed

Table 2. Summary of the Kinetic Data for the Reactions of Y-Substituted Phenyl Benzenesulfonates 5a–k with the Dissociated EtO^- and Ion-Paired EtOK in Anhydrous EtOH at 25.0 ± 0.1 °C[a]

entry	Y	pK_a	$10^3 k_{EtO^-}$/ M^{-1} s^{-1}	$10^3 k_{EtOK}$/ M^{-1} s^{-1}	k_{EtOK}/k_{EtO^-}
5a	2,4-$(NO_2)_2$	8.04	5820 ± 400	40600 ± 400	6.98
5b	3,4-$(NO_2)_2$	9.75	1400 ± 110	5700 ± 100	4.07
5c	4-NO_2	11.98	28.7[b]	137[b]	4.77
5d	4-CHO	12.66	3.28 ± 0.70	22.4 ± 0.4	6.83
5e	2,4-Cl_2	12.91	4.30 ± 1.00	54.6 ± 0.9	12.7
5f	4-CN	13.04	6.79 ± 0.60	66.3 ± 0.3	9.76
5g	4-COMe	13.26	2.56 ± 0.20	13.4 ± 0.1	5.23
5h	4-CF_3	13.76	2.69[b]	16.6[b]	6.17
5i	3-Br	14.54	1.10[b]	8.20[b]	7.45
5j	4-Cl	14.90	0.450[b]	3.50[b]	7.78
5k	H	15.76	0.0510[b]	0.520[b]	10.2

[a] pK_a data for Y-PhOH in EtOH were taken from ref 16. [b] The kinetic data for the reactions of **5c** and **5h–k** were taken from ref 13.

that k_{EtO^-} decreases as the leaving aryloxide becomes more basic; e.g., it decreases from 5.82 M^{-1} s^{-1} to 3.28 × 10^{-3} and 5.10 × 10^{-5} M^{-1} s^{-1} as the pK_a of the conjugate acid of the leaving aryloxide increases from 8.04 to 12.66 and 15.76, in turn. A similar result is demonstrated for the reactions with the ion-paired EtOK, although the ion-paired species is more reactive than the dissociated EtO^- in all cases. It is also noted that the k_{EtOK}/k_{EtO^-} ratio shows no correlation with the electronic nature of the substituent Y. This contrasts the preceding result; i.e., the k_{EtOK}/k_{EtO^-} ratio is linearly dependent on the electronic nature of the substituent X for the reactions of **4a–f** (Table 1 and Figure S1 in the SI). The contrasting K^+ ion effect will be discussed in detail in the following section.

The effect of the leaving-group basicity on the rate constants is illustrated in Figure 4. The Brønsted-type plots for the reactions of **5a–k** with the dissociated EtO^- and ion-paired EtOK are linear over 7 pK_a units with β_{lg} = −0.62 ± 0.02. Such linear Brønsted-type plots are contrasting to the curved Brønsted-type plots reported previously for the piperidinolysis of Y-substituted phenyl benzoates[19b] and quinuclidinolysis of diaryl carbonates (e.g., β_{lg} changes from −1.4 ± 0.1 to −0.3 ± 0.1 as the leaving group basicity decreases),[20] which were suggested to proceed through a stepwise mechanism with a change in the RDS.[20] The β_{lg} value of −0.6 ± 0.1 is typical of reactions reported previously to proceed through a concerted mechanism (e.g., β_{lg} = −0.52 for the reactions of aryl dimethylphosphinothioates with phenoxide anion,[21] β_{lg} = −0.54 for the alkaline ethanolysis of Y-substituted phenyl diphenylphosphinates,[22a] and β_{lg} = −0.66 for the reactions of aryl diphenylphosphinates with piperidine[22b]). Thus, one might suggest that the current reactions proceed through a concerted mechanism on the basis of the magnitude of the β_{lg} value shown in Figure 4.

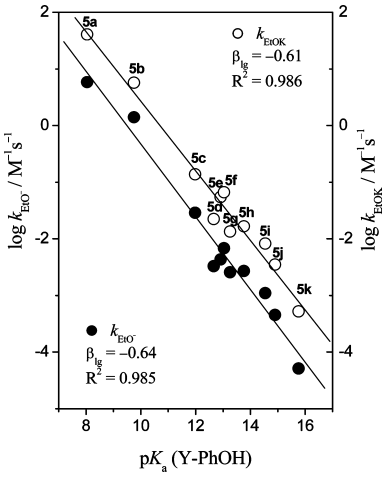

Figure 4. Brønsted-type plots for the reactions of Y-substituted phenyl benzenesulfonates **5a–k** with the dissociated EtO^- (●) and ion-paired EtOK (○) in anhydrous EtOH at 25.0 ± 0.1 °C. The identity of the points is given in Table 2.

Hammett plots constructed using σ° and σ^- constants are useful to study the reaction mechanism. If the current reactions proceed through a concerted mechanism as suggested above, breakdown of the S–OAr bond occurs at the RDS. In this case, a partial negative charge develops on the oxygen atom of the leaving aryloxide in the rate-determining TS. Since such negative charge can be delocalized to the substituent Y through resonance interactions, σ^- constants should give a better Hammett correlation than σ° constants. On the contrary, if the reaction proceeds through a stepwise mechanism, breakdown of the S–OAr bond should occur after the RDS. This is because EtO^- is much more basic and a poorer nucleofuge than the Y-substituted phenoxide ion. Accordingly, if the reaction proceeds through a stepwise mechanism, no negative charge would develop on the oxygen atom of the leaving aryloxide in the rate-determining TS. In this case, σ° constants should result in a better Hammett correlation than σ^- constants.

Thus, Hammett plots have been constructed using σ_Y^- and σ_Y° constants to examine whether the S–OAr bond rupture occurs in the RDS. As shown in Figure S2 in the SI, σ_Y° constants result in a better correlation than σ_Y^- constants for the reactions of **5b–d** and **5f–k** with the dissociated EtO^- (e.g., R^2 = 0.988 for σ_Y° and R^2 = 0.967 for σ_Y^- constants). A similar result is shown in Figure S3 in the SI for the reactions of **5b–d** and **5f–k** with the ion-paired EtOK (i.e., R^2 = 0.989 for σ_Y° and R^2 = 0.964 for σ_Y^- constants). This appears to indicate that no negative charge develops on the oxygen atom of the leaving aryloxide. Thus, one might suggest that the current reactions proceed through a stepwise mechanism, in which expulsion of the leaving group occurs after the RDS. Clearly, this is inconsistent with the concerted mechanism proposed in the preceding section on the basis of the linear Brønsted-type plots with β_{lg} = −0.6 but is consistent with our previous report that alkaline ethanolysis of Y-substituted phenyl benzenesulfonates (Y = 4-NO_2, 3-NO_2, 4-CF_3, 3-Br, 4-Cl, and H) proceeds through a stepwise mechanism.[13]

We suggest that the discrepancies in the reaction mechanisms may be due to the limited numbers of substituents to construct a Hammett plot with σ^- constants, because only 4-NO_2 has a σ^- constant among the 6 substituents studied previously.[13] In fact, a careful examination of Figures S2 and S3

dx.doi.org/10.1021/jo302373y | J. Org. Chem. 2013, 78, 490–497

in the SI reveals that the Hammett plots correlated with σ° constants also exhibit many scattered points. Thus, the conclusion drawn from the traditional Hammett correlation using σ° and σ^- constants is considered not to be reliable.

To obtain more conclusive information on the reaction mechanism, the dual-parameter Yukawa–Tsuno equation (eq 6) has been employed. Equation 6 was originally derived to account for the results obtained from solvolysis of benzylic systems, in which a partial positive charge develops in the TS.[23] We have recently shown that eq 6 is highly effective in elucidating ambiguities in the reaction mechanisms of benzenesulfonyl,[18] benzoyl[19] and phosphinyl[22] transfer reactions with amines or anionic nucleophiles.

$$\log(k_Y/k_H) = \rho_Y[\sigma_Y^\circ + r(\sigma_Y^- - \sigma_Y^\circ)] \quad (6)$$

Thus, Yukawa–Tsuno plots have been constructed in Figure 5 for the reactions of **5b–d** and **5f–k** with the dissociated EtO^-

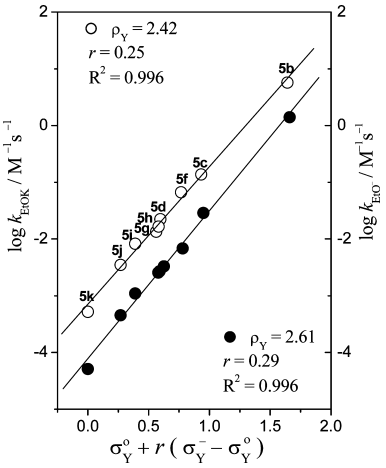

Figure 5. Yukawa–Tsuno plots for the reactions of Y-substituted phenyl benzenesulfonates **5b–d** and **5f–k** with the dissociated EtO^- (●) and ion-paired EtOK (○) in anhydrous EtOH at 25.0 ± 0.1 °C. The identity of the points is given in Table 2.

and ion-paired EtOK. The Yukawa–Tsuno plots exhibit excellent linear correlations with ρ_Y = 2.61 and r = 0.29 for the reactions with the dissociated EtO^- and ρ_Y = 2.42 and r = 0.25 for those with the ion-paired EtOK. Since the r value in the Yukawa–Tsuno equation represents the resonance demand of the reaction center or the extent of resonance contributions,[23,24] the r value of 0.25 or 0.29 obtained in this study indicates that a negative charge develops partially on the oxygen atom of the leaving aryloxide, which can be delocalized to the substituent Y through resonance interactions. This is only possible for reactions in which breakdown of the S–OAr bond occurs in the RDS. As discussed above, no negative charge would develop on the leaving group if the current reactions proceed through a stepwise mechanism. Thus, one can conclude that the current reactions proceed through a concerted mechanism, in which expulsion of the leaving group is advanced only slightly on the basis of the small r values. This is consistent with the preceding suggestion that the reactions of **5a–k** proceed through a concerted mechanism on the basis of the linear Brønsted-type plots with $\beta_{lg} = -0.6 \pm 0.1$.

Role of K^+ Ion: An Increase in Electrophilicity or Nucleofugality. One might expect that the TS structure for the reactions with the dissociated EtO^- is similar to TS_2, in which formation of the EtO–S bond and breakdown of the S–OAr bond occur simultaneously. It is noted that K^+ ion is absent in TS_2. In contrast, K^+ ion should be involved in the TS for the reactions with the ion-paired EtOK, since K^+ ion catalyzes the reactions. Thus, one can suggest that K^+ ion catalyzes the current reactions by increasing the electrophilicity of the reaction center through TS_3 or by increasing the nucleofugality of the leaving aryloxide through TS_4.

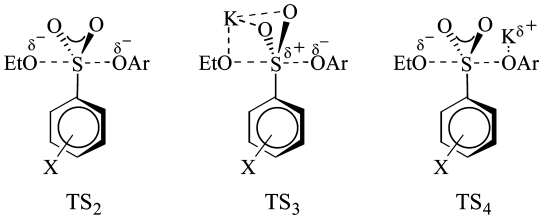

TS_2 TS_3 TS_4

If the reactions with the ion-paired EtOK proceed through TS_3, one might expect that the catalytic effect shown by K^+ ion (i.e., the k_{EtOK}/k_{EtO^-} ratio) is dependent on the electronic nature of the substituent X in the benzenesulfonyl moiety (proximal) but independent of the substituent Y in the leaving aryloxide (distal). On the contrary, if the reactions proceed through TS_4, the k_{EtOK}/k_{EtO^-} ratio would be independent of the substituent X (distal) but dependent on the substituent Y (proximal). In fact, the k_{EtOK}/k_{EtO^-} ratio decreases linearly as the substituent X changes from an EDG to an EWG (Table 1 and Figure S1 in the SI) but is independent of the substituent Y (Table 2). Thus, one can conclude that the reactions with the ion-paired EtOK proceed through TS_3, in which K^+ ion catalyzes the reactions by increasing the elctrophilicity of the reaction center.

Table 3. Summary of the Kinetic Results for the Reactions of 3,4-Dinitrophenyl Benzenesulfonate 5b, 4-Nitrophenyl Benzenesulfonate 5c, and 4-Cyanophenyl Benzenesulfonate 5f with the Dissociated EtO^- and Ion-Paired EtOK in Anhydrous EtOH at 5 Different Temperatures

	$10^3k_{EtO^-}/M^{-1}\ s^{-1}$						
	15.0 °C	20.0 °C	25.0 °C	30.0 °C	35.0 °C	$\Delta H^‡$/kcal mol^{-1}	$\Delta S^‡$/eu
5b	532 ± 20	761 ± 70	1400 ± 110	2460 ± 200	3310 ± 100	16.5 ± 1.0	−2.7 ± 0.2
5c	6.72 ± 1.00	17.1 ± 2.0	28.7	50.1 ± 4.0	84.2 ± 10.0	21.1 ± 1.4	5.1 ± 0.4
5f	1.24 ± 0.30	2.95 ± 1.00	6.79 ± 0.60	9.84 ± 2.00	20.7 ± 2.0	23.7 ± 1.6	10.2 ± 0.8
	$10^3k_{EtOK}/M^{-1}\ s^{-1}$						
	15.0 °C	20.0 °C	25.0 °C	30.0 °C	35.0 °C	$\Delta H^‡$/kcal mol^{-1}	$\Delta S^‡$/eu
5b	2680 ± 22	4260 ± 67	5700 ± 100	8800 ± 190	12000 ± 156	12.6 ± 0.5	−12.8 ± 0.4
5c	55.2 ± 1.0	84.3 ± 1.1	137	221 ± 3	309 ± 8	15.0 ± 0.4	−12.2 ± 0.4
5f	27.6 ± 0.2	45.4 ± 0.7	66.3 ± 0.3	111 ± 1	168 ± 1	15.3 ± 0.4	−12.4 ± 0.4

dx.doi.org/10.1021/jo302373y | J. Org. Chem. 2013, 78, 490–497

Activation Parameters and TS Structures. To further probe the above conclusion, activation parameters ($\Delta H^{\ddagger}$ and $\Delta S^{\ddagger}$) have been calculated from the rate constants measured at 5 different temperatures for the reactions of 3,4-dinitrophenyl benzenesulfonate **5b**, 4-nitrophenyl benzenesulfonate **5c**, and 4-cyanophenyl benzenesulfonate **5f** with the dissociated EtO^- and ion-paired EtOK. The kinetic results are summarized in Table 3 and illustrated graphically in Figure 6. The Arrhenius

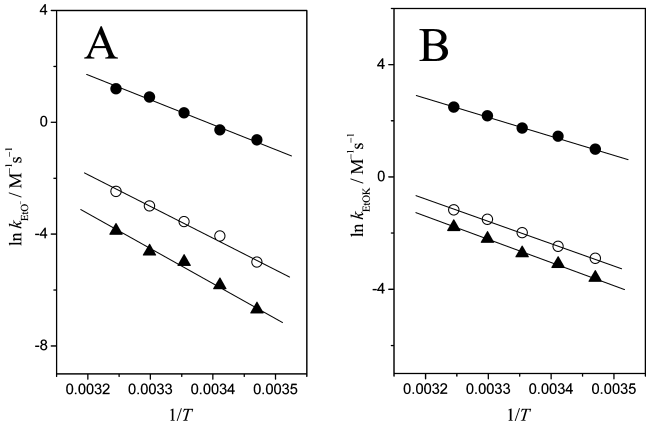

Figure 6. Arrhenius plots for the reactions of 3,4-dinitrophenyl benzenesulfonate **5b** (●), 4-nitrophenyl benzenesulfonate **5c** (○), and 4-cyanophenyl benzenesulfonate **5f** (▲) with the dissociated EtO^- (A) and ion-paired EtOK (B) in anhydrous EtOH at 25.0 ± 0.1 °C.

plots exhibit excellent linear correlations for the reactions with the dissociated EtO^- and ion-paired EtOK, indicating that the $\Delta H^{\ddagger}$ and $\Delta S^{\ddagger}$ values determined in this way are reliable.

It is apparent that the electronic nature of substituent Y in the leaving group influences the bond dissociation energy of the S−OAr bond. Furthermore, the energy required to break the S−OAr bond is reflected in the $\Delta H^{\ddagger}$. Thus, one might expect that the $\Delta H^{\ddagger}$ in the current reactions is dependent on the electronic nature of the substituent Y (e.g., σ_Y constants) if breakdown of the S−OAr bond occurs in the RDS. In fact, Table 3 and Figure S4 in the SI show that the $\Delta H^{\ddagger}$ values for the reactions with the dissociated EtO^- and ion-paired EtOK are strongly dependent on the electronic nature of the substituent Y (e.g., slope = −7.17 and R^2 = 0.995 for the reactions with the dissociated EtO^- and slope = −2.88 and R^2 = 0.985 for the reactions with the ion-paired EtOK). Such strong dependence of $\Delta H^{\ddagger}$ on the electronic nature of the substituent Y would be only possible for reactions in which breakdown of the S−OAr bond occurs in the RDS. This idea further supports the preceding conclusion that the current reactions proceed through a concerted mechanism with TS structures similar to TS_2 and TS_3 for the reactions with the dissociated EtO^- and ion-paired EtOK, respectively.

The above argument is further supported by the $\Delta S^{\ddagger}$ values. Table 3 shows that the $\Delta S^{\ddagger}$ for the reactions with the dissociated EtO^- is strongly dependent on the electronic nature of the substituent Y; i.e., it increases from −2.7 eu to +5.1 and +10.2 eu as the substituent Y in the leaving group changes from 3,4-$(NO_2)_2$ to 4-NO_2 and 4-CN, in turn. In contrast, the $\Delta S^{\ddagger}$ for the reactions with the ion-paired EtOK remains nearly constant at −12.5 ± 0.4 eu regardless of the electronic nature of the substituent Y. The contrasting $\Delta S^{\ddagger}$ behaviors can be attributed to the structural difference between TS_2 and TS_3. It is evident that TS_3 would experience some restrictions in the rotational and vibrational degrees of freedom due to its cyclic structure, while such restrictions are absent in TS_2. This idea is in accord with the fact that the $\Delta S^{\ddagger}$ values are significantly more negative for the reactions with the ion-paired EtOK than for those with the dissociated EtO^-.

One might suggest that differential solvation of the GS and TS is responsible for the result that $\Delta S^{\ddagger}$ for the reactions with the dissociated EtO^- is linearly dependent on the nature of the substituent Y (see also Figure S5 in the SI). It is expected that the dissociated EtO^- is strongly solvated in EtOH through H-bonding interactions. Since the negative charge of the EtO^- ion in the GS is partially transferred to the electrophilic center of the substrate in the TS, solvation of the TS (i.e., TS_2) through H-bonding interactions would decrease. Thus, one might expect an increase in $\Delta S^{\ddagger}$ due to a decrease in solvation of the TS. Furthermore, the charge transfer from EtO^- to the electrophilic center in the TS would be more advanced for the reaction in which formation of the EtO−S bond is more advanced in the TS. Therefore, $\Delta S^{\ddagger}$ is expected to increase more significantly for the reaction that proceeds through a later TS (or for the reaction of the substrate possessing a weaker EWG on the basis of a normal Hammond effect).[25] In fact, $\Delta S^{\ddagger}$ increases from −2.7 eu to +5.1 and +10.2 eu as the substituent Y changes from 3,4-$(NO_2)_2$ to 4-NO_2 and 4-CN, in turn (Table 3).

However, such solvation effect is expected to be less important for the reactions with the ion-paired EtOK than for those with the dissociated EtO^- since the ion-paired species would be less strongly solvated than the dissociated one. Thus, the $\Delta S^{\ddagger}$ value would be influenced mainly by the degrees of bond formation and bond rupture in the TS. One might expect that the reaction of the substrate possessing a weaker EWG in the leaving group (or the less reactive substrate) would proceed through a later TS; i.e., both formation of the EtO−S bond and breakdown of the S−OAr bond would be more advanced as the substituent Y in the leaving aryloxide changes from 3,4-$(NO_2)_2$ to 4-NO_2 or to 4-CN. It is obvious that $\Delta S^{\ddagger}$ decreases with increasing the degree of the EtO−S bond formation but increases with increasing the degree of the S−OAr bond rupture. Accordingly, decreased $\Delta S^{\ddagger}$ upon formation of the EtO−S bond would be compensated by increased $\Delta S^{\ddagger}$ upon breakdown of the S−OAr bond. This accounts nicely for the result shown in Table 3 that the $\Delta S^{\ddagger}$ values are practically the same for the reactions **5b**, **5c** and **5f** with the ion-paired EtOK. Thus, the contrasting $\Delta S^{\ddagger}$ values for the reactions with the dissociated EtO^- and ion-paired EtOK also support the proposed TS structures (i.e., TS_2 and TS_3, respectively).

■ CONCLUSIONS

Analyses of the kinetic data through LFERs and activation parameters have led us to draw the following conclusions: (1) The Brønsted-type plots for the reactions of **5a**−**k** with the dissociated EtO^- and ion-paired EtOK are linear with β_{lg} = −0.62 ± 0.02, a typical β_{lg} value for the reactions reported previously to proceed through a concerted mechanism. The linear Yukawa−Tsuno plots with ρ_Y = 2.42−2.61 and r = 0.25−0.29 also suggest that the reactions proceed through a concerted mechanism, in which breakdown of the S−OAr bond is advanced only slightly. (2) The k_{EtOK}/k_{EtO^-} ratio is strongly dependent on the electronic nature of the substituent X in the benzenesulfonyl moiety but is independent of the substituent Y in the leaving group, implying that K^+ ion catalyzes the reactions by increasing the electrophilicity of the

dx.doi.org/10.1021/jo302373y | J. Org. Chem. 2013, 78, 490−497

reaction center through TS_3 rather than by increasing the nucleofugality of the leaving group through TS_4. (3) The concerted mechanism is further supported by the fact that the $\Delta H^{\ddagger}$ values for the reactions with the dissociated EtO^- and ion-paired EtOK are linearly dependent on the electronic nature of the substituent Y. (4) The reactions with the ion-paired EtOK result in more negative $\Delta S^{\ddagger}$ values than those with the dissociated EtO^-. Restrictions of the rotational and vibrational degrees of freedom in the cyclic TS_3 are responsible for the more negative $\Delta S^{\ddagger}$ values. (5) The $\Delta S^{\ddagger}$ value is strongly dependent on the electronic nature of the substituent Y for the reactions with the dissociated EtO^- but remains nearly constant for the reactions with the ion-paired EtOK. The difference in structures between TS_2 and TS_3 is responsible for the contrasting $\Delta S^{\ddagger}$ behaviors.

EXPERIMENTAL SECTION

Materials. Compounds **4a**−**f** were prepared readily from the reaction of 2,4-dinitrophenol and X-substituted benzenesulfonyl chloride in the presence of triethylamine in anhydrous ether, while **5a**−**k** were synthesized from the reaction of benzenesulfonyl chloride with the respective Y-substituted phenol, as reported previously.[18] The crude products were purified by column chromatography, and their purity was checked by their melting points and ^1H NMR spectra. EtOK stock solution was prepared by dissolving potassium metal in anhydrous ethanol under N_2 and stored in a refrigerator. The concentration of EtOK was measured by titration with monopotassium phthalate. The anhydrous ethanol was further dried over magnesium and distilled under N_2 just before use.

Kinetics. Kinetic studies were performed with a UV−vis spectrophotometer for slow reactions ($t_{1/2} \geq 10$ s) or with a stopped-flow spectrophotometer for fast reactions ($t_{1/2} < 10$ s) equipped with a constant-temperature circulating bath. The reactions were followed by monitoring the appearance of the Y-substituted phenoxide ion. Reactions were followed generally for 9 half-lives, and k_{obsd} were calculated using the equation $\ln (A_\infty - A_t)$ vs t. The plots of $\ln (A_\infty - A_t)$ vs t were linear over 90% of the total reaction.

Typically, the reaction was initiated by adding 5 μL of a 0.02 M solution of 2,4-dinitrophenyl benzenesulfonate in acetonitrile to a 10 mm quartz UV cell containing 2.50 mL of the thermostatted reaction mixture made of the solvent EtOH and an aliquot of the EtOK stock solution. All solutions were transferred by gastight syringes. Generally, the EtOK concentration was varied over the range $(2-100) \times 10^{-3}$ M, while the substrate concentration was ca. 4×10^{-5} M.

Products Analysis. Y-Substituted phenoxide was liberated quantitatively and identified as one of the products by comparison of the UV−vis spectrum after completion of the reaction with that of the authentic sample under the same reaction conditions.

ASSOCIATED CONTENT

Supporting Information

Plot of log (k_{EtOK}/k_{EtO^-}) vs σ_x for the reactions of 2,4-dinitrophenyl X-substituted benzenesulfonates **4a**−**f** with EtOK (Figure S1); Hammett plots correlated with σ_Y^- and σ_Y° constants for the reactions of Y-substituted phenyl benzenesulfonates **5b**−**d** and **5f**−**k** with the dissociated EtO^- and ion-paired EtOK (Figures S2 and S3); plots of $\Delta H^{\ddagger}$ vs σ_Y^- constants for the reactions of 3,4-dinitrophenyl benzenesulfonate **5b**, 4-nitrophenyl benzenesulfonate **5c**, and 4-cyanophenyl benzenesulfonate **5f** with the dissociated EtO^- and ion-paired EtOK (Figure S4); plot of $\Delta S^{\ddagger}$ vs σ_Y^- constants for the reactions of 3,4-dinitrophenyl benzenesulfonate **5b**, 4-nitrophenyl benzenesulfonate **5c**, and 4-cyanophenyl benzenesulfonate **5f** with the dissociated EtO^- (Figure S5); plots of k_{obsd} vs [EtOK] and $k_{obsd}/[EtO^-]_{eq}$ vs $[EtO^-]_{eq}$ in Figures S6−S27. The k_{obsd} values and detailed kinetic conditions (Tables S1−S23). This material is available free of charge via the Internet at http://pubs.acs.org.

AUTHOR INFORMATION

Corresponding Author

*E-mail: ihum@ewha.ac.kr.

Notes

The authors declare no competing financial interest.

ACKNOWLEDGMENTS

This research was supported by the Basic Science Research Program through the National Research Foundation of Korea (NRF) funded by the Ministry of Education, Science and Technology (2012-R1A1B3001637), and by NSERC of Canada (E.B.). Ji-Sun Kang is also grateful for the BK 21 Scholarship as well as the scholarship provided by the Lotte Foundation.

REFERENCES

(1) (a) Mohamed, M. F.; Sanchez-Lombardo, I.; Neverov, A. A.; Brown., R. S. *Org. Biomol. Chem.* **2012**, *10*, 631−639. (b) Barrera, I. F.; Maxwell, C. I.; Neverov, A. A.; Brown, R. S. *J. Org. Chem.* **2012**, *77*, 4156−4160. (c) Raycroft, M. A. R.; Liu, C. T.; Brown, R. S. *Inorg. Chem.* **2012**, *51*, 3846−3854. (d) Brown, R. S. *Prog. Inorg. Chem.* **2012**, *57*, 55−117. (e) Dhar, B. B.; Edwards, D. R.; Brown, R. S. *Inorg. Chem.* **2011**, *50*, 3071−3077. (f) Edwards, D. R.; Neverov, A. A.; Brown, R. S *Inorg. Chem.* **2011**, *50*, 1786−1797. (g) Brown, R. S.; Lu, Z. L.; Liu, C. T.; Tsang, W. Y.; Edwards, D. R.; Neverov., A. A. *J. Phys. Org. Chem.* **2010**, *23*, 1−15. (h) Mohamed, M. F.; Neverov, A. A.; Brown., R. S. *Inorg. Chem.* **2009**, *48*, 11425−11433. (i) Brown, R. S.; Neverov, A. A. *Adv. Phys. Org. Chem.* **2007**, *42*, 271−331.

(2) (a) Feng, G.; Tanifum, E. A.; Adams, H.; Hengge, A. C. *J. Am. Chem. Soc.* **2009**, *131*, 12771−12779. (b) Humphry, T.; Iyer, S.; Iranzo, O.; Morrow, J. R.; Richard, J. P.; Paneth, P.; Hengge, A. C. *J. Am. Chem. Soc.* **2008**, *130*, 17858−17866. (c) Zalatan, J. G.; Catrina, I.; Mitchell, R.; Grzyska, P. K.; O'Brien, P. J.; Herschlag, D.; Hengge, A. C. *J. Am. Chem. Soc.* **2007**, *129*, 9789−9798. (d) Davies, A. G. *J. Chem. Res.* **2008**, 361−375. (e) Davies, A. G. *Perkin* **2000**, *1*, 1997−2010.

(3) (a) Chei, W. S.; Ju, H.; Suh, J. *Bioorg. Med. Chem. Lett.* **2012**, *22*, 1533−1537. (b) Chei, W. S.; Ju, H.; Suh, J. *J. Biol. Inorg. Chem.* **2011**, *16*, 511−519. (c) Kim, H. M.; Jang, B.; Cheon, Y. E.; Suh, M. P.; Suh, J. *J. Biol. Inorg. Chem.* **2009**, *14*, 151−157. (d) Chei, W. S.; Suh, J. *Prog. Inorg. Chem.* **2007**, *55*, 79−142. (e) Jeung, C. S.; Song, J. B.; Kim, Y. H.; Suh, J. *Bioorg. Med. Chem. Lett.* **2001**, *11*, 3061−3064. (f) Suh, J.; Son, S. J.; Suh, M. P. *Inorg. Chem.* **1998**, *37*, 4872−4877. (g) Suh, J.; Kim, N.; Cho, H. S. *Bioorg. Med. Chem. Lett.* **1994**, *4*, 1889−1892. (h) Suh, J. *Acc. Chem. Res.* **1992**, *25*, 273−279.

(4) (a) Lee, J. H.; Park, J.; Lah, M. S.; Chin, J.; Hong, J. I. *Org. Lett.* **2007**, *9*, 3729−3731. (b) Livieri, M.; Manicin, F.; Saielli, G.; Chin, J.; Tonellato, U. *Chem.—Eur. J.* **2007**, *13*, 2246−2256. (c) Livieri, M.; Mancin, F.; Tonellato, U.; Chin, J. *Chem. Commun.* **2004**, 2862−2863. (d) Williams, N. H.; Takasaki, B.; Wall, M.; Chin, J. *Acc. Chem. Res.* **1999**, *32*, 485−493.

(5) (a) Nielsen, L. P. C.; Zuend, S. J.; Ford, D. D.; Jacobsen, E. N. *J. Org. Chem.* **2012**, *77*, 2486−2495. (b) Fife, T. H.; Chauffe, L. *Bioorg. Chem.* **2000**, *28*, 357−373. (c) Fife, T. H.; Bembi, R. *J. Am. Chem. Soc.* **1993**, *115*, 11358−11363. (d) Fife, T. H.; Pujari, M. P. *J. Am. Chem. Soc.* **1990**, *112*, 5551−5557.

(6) (a) Buncel, E.; Dunn, E. J.; Bannard, R. B.; Purdon, J. G. *J. Chem. Soc., Chem. Commun.* **1984**, 162−163. (b) Dunn, E. J.; Buncel, E. *Can. J. Chem.* **1989**, *67*, 1440−1448. (c) Pregel, M. J.; Dunn, E. J.; Nagelkerke, R.; Thatcher, G. R. J.; Buncel, E. *Chem. Soc. Rev.* **1995**, *24*, 449−455.

(7) (a) Koo, I. S.; Ali, D.; Yang, K.; Park, Y.; Esbata, A.; van Loon, G. W.; Buncel, E. *Can. J. Chem.* **2009**, *87*, 433−439. (b) Buncel, E.; Albright, K. G.; Onyido, I. *Org. Biomol. Chem.* **2005**, *3*, 1468−1475. (c) Buncel, E.; Albright, K. G.; Onyido, I. *Org. Biomol. Chem.* **2004**, *2*, 601−610. (d) Nagelkerke, R.; Thatcher, G. R. J.; Buncel, E. *Org.*

Biomol. Chem. **2003**, *1*, 163−167. (e) Buncel, E.; Nagelkerke, R.; Thatcher, G. R. J. *Can. J. Chem.* **2003**, *81*, 53−63.
(8) (a) Hoepker, A. C.; Collum, D. B. *J. Org. Chem.* **2011**, *76*, 7985−7993. (b) Cacciapaglia, R.; Mandolini, L. *Chem. Soc. Rev.* **1993**, *22*, 221−231. (c) Cacciapaglia, R.; Mandolini, L.; Tomei, A. *J. Chem. Soc., Perkin Trans.* **1994**, *2*, 367−372. (d) Cacciapaglia, R.; Van Doorn, A. R.; Mandolini, L.; Reinhoudt, D. N.; Verboom, W. *J. Am. Chem. Soc.* **1992**, *114*, 2611−2617. (e) Cacciapaglia, R.; Mandolini, L.; Reinhoudt, D. N.; Verboom, W. *J. Phys. Org. Chem.* **1992**, *5*, 663−669.
(9) Um, I. H.; Shin, Y. H.; Park, J. E.; Kang, J. S.; Buncel, E. *Chem.—Eur. J.* **2012**, *18*, 961−968.
(10) (a) Um, I. H.; Shin, Y. H.; Lee, S. E.; Yang, K. Y.; Buncel, E. *J. Org. Chem.* **2008**, *73*, 923−930. (b) Um, I. H.; Jeon, S. E.; Baek, M. H.; Park, H. R. *Chem. Commun.* **2003**, 3016−3017.
(11) (a) Martin, D. W.; Mayes, P. A.; Rodwell, V. W.; Granner, D. K. *Harper's Review of Biochemistry*, 20th ed.; Lange Medical Publications: Los Altos, CA, 1985; p 630. (b) Dugas, H. *Bioorganic Chemistry*, 2nd ed.; Springer-Verlag: New York, 1989; p 284.
(12) Eisenman, G. *Biophys. J.* **1962**, *2*, 259−323.
(13) Pregel, M. J.; Dunn, E. J.; Buncel., E. *J. Am. Chem. Soc.* **1991**, *113*, 3545−3550.
(14) Pechanec, V.; Kocian, O.; Zavada, J. *Collect. Czech. Chem. Commun.* **1982**, *47*, 3405−3411.
(15) Barthel, J.; Justice, J.-C.; Wachter, R. *Z. Phys. Chem.* **1973**, *84*, 100−113.
(16) Um, I. H.; Hong, Y. J.; Kwon, D. S. *Tetrahedron* **1997**, *53*, 5073−5082.
(17) Um, I. H.; Kim, E. H.; Lee, J. Y. *J. Org. Chem.* **2009**, *74*, 1212−1217.
(18) Um, I. H.; Chun, S. M.; Chae, O. M.; Fujio, M.; Tsuno, Y. *J. Org. Chem.* **2004**, *69*, 3166−3172.
(19) (a) Um, I. H.; Bae, A. R. *J. Org. Chem.* **2011**, *76*, 7510−7515. (b) Um, I. H.; Lee, J. Y.; Ko, S. H.; Bae, S. K. *J. Org. Chem.* **2006**, *71*, 5800−5803. (c) Um, I. H.; Kim, K. H.; Park, H. R.; Fujio, M.; Tsuno, Y. *J. Org. Chem.* **2004**, *69*, 3937−3942. (d) Um, I. H.; Lee, S. E.; Kwon, H. J. *J. Org. Chem.* **2002**, *67*, 8999−9005.
(20) (a) Gresser, M. J.; Jencks, W. P. *J. Am. Chem. Soc.* **1977**, *99*, 6963−6970. (b) Gresser, M. J.; Jencks, W. P. *J. Am. Chem. Soc.* **1977**, *99*, 6970−6980.
(21) Onyido, I.; Swierczek, K.; Purcell, J.; Hengge, A. C. *J. Am. Chem. Soc.* **2005**, *127*, 7703−7711.
(22) (a) Um, I. H.; Park, J. E.; Shin, Y. H. *Org. Biomol. Chem.* **2007**, *5*, 3539−3543. (b) Um, I. H.; Shin, Y. H.; Han, J. Y.; Mishima, M. *J. Org. Chem.* **2006**, *71*, 7715−7720.
(23) (a) Tsuno, Y.; Fujio, M. *Adv. Phys. Org. Chem.* **1999**, *32*, 267−385. (b) Tsuno, Y.; Fujio, M. *Chem. Soc. Rev.* **1996**, *25*, 129−139. (c) Yukawa, Y.; Tsuno, Y. *Bull. Chem. Soc. Jpn.* **1959**, *32*, 965−970.
(24) (a) Than, S.; Badal, M.; Itoh, S.; Mishima, M. *J. Phys. Org. Chem.* **2010**, *23*, 411−417. (b) Itoh, S.; Badal, M.; Mishima, M. *J. Phys. Chem. A* **2009**, *113*, 10075−10080. (c) Than, S.; Maeda, H.; Irie, M.; Kikukawa, K.; Mishima, M. *Int. J. Mass Spectrom.* **2007**, *263*, 205−214. (d) Maeda, H.; Irie, M.; Than, S.; Kikukawa, K.; Mishima, M. *Bull. Chem. Soc. Jpn.* **2007**, *80*, 195−203. (e) Fujio, M.; Alam, M. A.; Umezaki, Y.; Kikukawa, K.; Fujiyama, R.; Tsuno, Y. *Bull. Chem. Soc. Jpn.* **2007**, *80*, 2378−2383.
(25) Hammond, G. S. *J. Am. Chem. Soc.* **1955**, *77*, 334−338.